

High magnetic field induced phases and half-magnetization plateau in the $S = 1$ kagome compound $\text{Ni}_3\text{V}_2\text{O}_8$

Junfeng Wang,^{1,2} M. Tokunaga,¹ Z. Z. He,³ J. I. Yamaura,¹ A. Matsuo,¹ and K. Kindo¹

¹The Institute for Solid State Physics (ISSP), The University of Tokyo, Chiba 277-8581, Japan

²Wuhan National High Magnetic Field Center, Huazhong University of Science and Technology, Wuhan 430074, China

³State Key Laboratory of Structural Chemistry, Fujian Institute of Research on the Structure of Matter, Chinese Academy of Sciences, Fuzhou, Fujian 350002, China

(Received 14 July 2011; published 19 December 2011)

We report on high magnetic field studies of magnetization, electric polarization, and specific heat on single crystals of $\text{Ni}_3\text{V}_2\text{O}_8$, which is an $S = 1$ kagome compound. The magnetization process exhibits multistep magnetic transitions when the magnetic field is parallel to the magnetic easy axis. An apparent magnetization plateau was observed at half the height of the saturation magnetization $M_s \sim 2.39\mu_B/\text{Ni}$. In addition, the magnetization transitions at higher fields are quantized at $2/3$, $3/4$, and $8/9$ of M_s . These results are unusual for the one-third magnetization plateaus that theories have predicted for conventional kagome antiferromagnets. We find that the high magnetic field suppresses the spontaneous polarization, leading to a different high-field phase where the magnetic structure is collinear or coplanar with the underlying lattice. The resulting high-field phase diagram explores several magnetic phases and sheds light on recent experimental findings. Analytical arguments have been presented to discuss these high-field phases.

DOI: 10.1103/PhysRevB.84.220407

PACS number(s): 75.10.Jm, 75.30.Kz

In magnetic materials, geometrical frustration generates a variety of nontrivial ordered states with peculiar spin correlations. Typical frustrated systems are the two-dimensional (2D) triangular and kagome (corner-sharing triangles) antiferromagnets. Many interesting aspects have been extensively studied in the past decade, such as the spin-liquid-like ground state,^{1,2} magnetically driven ferroelectric state,³ supersolid state,⁴ and magnetization plateaus.⁵

The problem of magnetization plateaus is more general because it also exists in one-dimensional (1D) and three-dimensional (3D) spin systems. The magnetization plateau is due to a field-driven ordered ground state where the magnetization shows field independence in a finite field range. This plateau and the saturation magnetization M_s are associated with a fractional value $m = M/M_s$, which satisfies the necessary condition $n(S - m) = \text{integer}$,⁵ where S is the spin and n is the magnetic periodicity. Note that not all the values that satisfy the condition will appear as a magnetization plateau. A well-known example is the appearance of a half- ($m = 1/2$) magnetization plateau in 1D quantum spin systems with $n = 2$. This plateau has been studied theoretically and experimentally in bond-alternating chains,⁶ ladders,⁷ and other spin chains.⁸ The $1/2$ plateau has also been realized in 3D classical spin systems, for example, Cr-based pyrochlore lattices where $n = 4$, with an “up-up-up-down” (*uud*) spin arrangement.⁹

For triangular and kagome lattices in which n is considered to be 3, the $1/2$ plateau is not expected due to the arguments given above. Instead, one-third ($m = 1/3$) plateaus appeared in triangular antiferromagnets.^{10–12} In the classical spin system, this $1/3$ -plateau phase has a collinear “up-up-down” (*uud*) spin arrangement for each triangle, while this state of the quantum case has a related *uud* spin configuration with the quantum fluctuation. This has been studied, for instance, in the materials CuFeO_2 ,¹⁰ $\text{RbFe}(\text{MoO}_4)_2$, $\text{CsFe}(\text{SO}_4)_2$,¹¹ etc., and for a quantum case of Cs_2CuBr_4 .¹² All of these

exhibited $1/3$ plateaus, as the theory predicted. In case of the analogous kagome lattices, similar $1/3$ plateaus have been predicted for the $S = 1$ and $1/2$ isotropic Heisenberg antiferromagnets by methods of numerical diagonalization,¹³ and for the easy-axis $S \geq 1$ kagome antiferromagnets by analytical arguments.^{14,15} Experimentally, however, to the best of our knowledge, no clear evidence shows a $1/3$ plateau in any kagome compound so far, although a weak $1/3$ -plateau-like anomaly was observed in the Cr-jarosite without saturation of the magnetization.¹⁶ Very recently, high-field magnetization studies of volborthite and vesignieite found plateaus toward 68 T at $m = 0.4$, higher than the predicted $1/3$ plateau.¹⁷ More surprisingly, a $1/2$ -plateau-like step was detected recently in the quantum magnet *m*-N-methylpyridinium nitronyl nitroxide (*m*-MPYNN)·BF₄.¹⁸ With a view to these results, it would be desirable to uncover more unconventional features in other kagome compounds in order to verify the theoretical predictions. In this Rapid Communication, we performed high-field magnetization studies on the Ni-based $S = 1$ kagome compound $\text{Ni}_3\text{V}_2\text{O}_8$ (NVO). We found that the magnetization process of NVO showed multistep transitions when the magnetic field was parallel to the magnetic easy axis, and finally saturated up to 48 T (Fig. 1). We observed an apparent magnetization plateau at half the height of the saturation magnetization M_s , together with other fractional magnetization transitions at higher fields.

The magnetic behavior of NVO is dominated by $S = 1$ Ni^{2+} ions. Two nonequivalent Ni^{2+} sites called spine and cross-tie spins form a special kagome-staircase geometry in the *ac* plane and stack along the *b* axis with an orthorhombic structure (*Cmca*), as illustrated in the inset of Fig. 1. The magnetic kagome planes are separated by nonmagnetic VO_4 tetrahedra, while within the kagome planes the Ni^{2+} ions interact with each other through Ni-O-O-Ni superexchange pathways. This compound is very attractive due to the anisotropic phase diagrams and complex magnetoelectric interactions.^{3,19–24} As

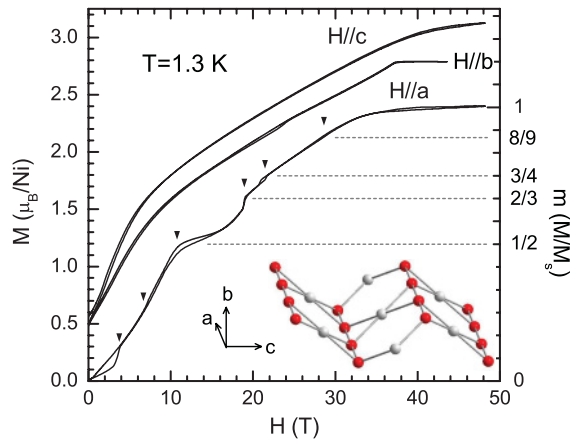


FIG. 1. (Color online) High-field magnetization processes at 1.3 K. The curves for $H \parallel b$ and $H \parallel c$ are lifted by $0.5\mu_B$ for clarity. Triangle symbols indicate various magnetic transitions. The dotted lines indicate the fractional values of M/M_s . The corresponding dM/dH data (for $H \parallel a$) are shown in Fig. 2. Inset: Kagome-staircase plane showing the spine (red/dark gray) and the cross-tie (gray) Ni^{2+} ions.

temperature (T) is lowered below 9.3 K, four magnetic ordered states occur subsequently, known as two incommensurate (called HTI and LTI) phases and two commensurate (called C and C') phases. These were explained as a competing result of the nearest-neighbor and next-nearest-neighbor interactions, anisotropy, Dzyaloshinskii-Moriya (DM) interactions, and pseudodipolar interactions.¹⁹ The LTI phase was confirmed to break the spatial inversion symmetry and generate spontaneous electric polarization.³ Polarized magnetic neutron diffraction demonstrated a strong coupling between magnetic and ferroelectric domains by electrical control of the cycloidal handedness.²⁰ Nevertheless, recent works in the low-field regions resulted in controversies and would imply different types of magnetism in this system.^{21,22} This has provided the motivation for using sufficiently high magnetic fields to reveal possible unique interactions or transitions. A successful example is that a different high-field state was revealed by a magneto-optical study up to 30 T for $H \parallel b$.²³ To the best of our knowledge, there are no studies of the high magnetic field of NVO, especially for the magnetic easy axis, i.e., $H \parallel a$. For these reasons, we performed high-field magnetization and electric polarization measurements up to 48 T on NVO single crystals.

High-quality transparent NVO single crystals were grown by the flux method.²⁴ Suitable crystals were selected and cut for the high-field magnetization, electric polarization, and specific-heat measurements. The pulsed magnet employed for the high-field studies has a short pulse duration of 7 ms. High-field magnetization was detected by the induction method with a coaxial pickup coil. The field-dependent electric polarization was derived from integrating the polarization current that was detected. Specific heat was measured using a commercial 14-T physical properties measurement system (PPMS). Low-field magnetization was measured by means of a 7-T superconducting quantum interference device (SQUID) magnetometer [magnetic property measurement system (MPMS)] and a 16-T [vibrating sample magnetometer (VSM)] PPMS.

Figure 1 displays the high-field magnetization data at 1.3 K. The magnetization processes along the three crystallographic axes are different due to the magnetic anisotropy. For $H \parallel c$, the M - H curve shows a small jump at 2 T and a hysteresis below 6 T. Then the slope decreases and the subsequent curve is almost linear up to 48 T without going into saturation. The hysteresis is supposed to arise from the weak ferromagnetic moment along c . For $H \parallel b$, a similar jump at 3 T and change of slope at ~ 8 T are observed. With increasing field, a robust saturation plateau appears above 37 T, indicative of the low-dimensional character of NVO along b . The low-field processes for the b and c axes can be understood as the crossover from phase C' to C according to previous phase diagrams.¹⁹ It should be noted that the 24-T anomaly for $H \parallel b$ is rather complex; this will be investigated in a separate paper. The most impressive observation in Fig. 1 is given by the successive magnetic transitions for $H \parallel a$. Distinct magnetization transitions are observed at $H_{c1} \sim 3$ T, $H_{c3} = 11$ T, $H_{c4} = 18$ T, and $H_{c5} = 22$ T, respectively. Other small transitions are sensitively detected in the dM/dH curve at $H_{c2} = 7$ T and $H_{c6} = 28$ T (see Fig. 2).²⁵ These transitions are not expected from the previous phase diagram for $H \parallel a$, implying the existence of different high-field states. A crucial finding is that a magnetization plateau apparently appears at $H_{c3} < H < H_{c4}$. The magnetization is exactly half the height of the saturation magnetization M_s of $\sim 2.39\mu_B/\text{Ni}$, which is close to the expected value using a g factor of 2.3.¹⁹ Moreover, other magnetization transitions are visible at $m = 2/3, 3/4,$

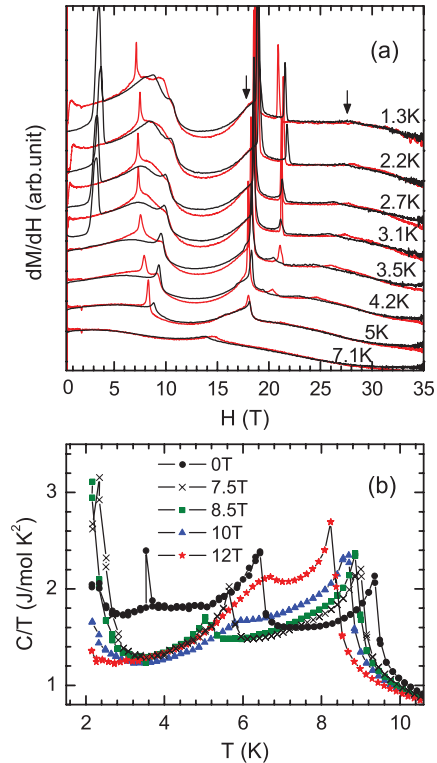


FIG. 2. (Color online) (a) Temperature dependence of dM/dH vs H for $H \parallel a$. The black (red or dark gray) curve is for increasing (decreasing) field. The data are vertically offset for clarity. The arrows indicate the small transitions at 1.3 K. (b) Magnetic specific heat for $H \parallel a$.

and 8/9. To check the low-field values of M , we have carried out steady field measurements up to 16 T and down to 2 K (not shown here), and find good agreement with our pulsed field data.

The appearance of a half-magnetization plateau is quite puzzling. It is hard to imagine how three spins can result in a 1/2-plateau phase on each triangle. Also, to the best of our knowledge, there has been no reported theory that predicted a 1/2 plateau in any spin system based on the kagome lattice. Since 1/2 plateaus may appear in 1D or 3D spin systems, it is reasonable to compare these to reexamine the peculiar kagome lattice of NVO. In the 1D case, the NVO kagome lattice can be decomposed into the spine spin chains and the cross-tie spin chains. The measurement of the incommensurate wave vector in phases HTI and LTI by neutron-diffraction experiments determined the ratio J_1/J_2 of nearest- and next-nearest-neighbor interaction along the spine spin chains to be 2.55.¹⁹ The spine spin chains in this J_1 - J_2 model can then be regarded as bond-alternating or dimer spin chains, which can yield a 1/2 plateau. However, because the cross-tie spins are frustrated in zero mean field with isotropic interactions, we could not expect them to contribute to a 1/2 plateau. For a 3D case, the interlayer interactions have to be considered. A first-principles calculation showed surprisingly strong interactions between adjacent kagome planes.²⁶ Thus we could expect a $uuud$ spin arrangement through adjacent kagome planes. Even so, the magnetic transitions at $m = 2/3$, $3/4$, and $8/9$ are not explained by this model.

Okamoto¹⁷ pointed out a way to explain the deviation of a magnetization plateau from the theoretical prediction, which means the preceding magnetic transitions before the plateau significantly enhance the magnetization and therefore result in excess magnetization. In fact, two other kagome compounds, $\text{Nd}_3\text{Ga}_5\text{SiO}_{14}$ and m -MPYNN· BF_4 , also exhibited features of 1/2 plateaus,^{2,18} although these have different kagome-lattice geometries. We note that a 3/4-plateau-like anomaly was found in m -MPYNN· BF_4 , which shows more similarity to our result. We note that the 1/2 plateau of NVO involves a phenomenon that is very similar to the so-called ‘‘magnetization ramp,’’ which was predicted for the 1/3 plateau of the kagome lattice by a recent numerical diagonalization study.²⁷ These facts provide evidence that the 1/2 plateau of NVO should be intrinsic, probably reflecting an ordered state involving the cross-tie spins. Hida²⁸ presented a ‘‘hexagonal singlet solid picture’’ for the ground state of $S = 1$ kagome Heisenberg antiferromagnets and applied it to m -MPYNN· BF_4 . In this model, the $S = 1$ spin was decomposed into two $S = 1/2$ spins which form singlet states with neighbors on each triangle yielding zero net moment, as expected from a VBS picture. Then, a possible 1/2-plateau state of NVO will show that one half of the number of triangles has these spin singlet states, while the others remain as triplet $S = 1$ along the applied magnetic field, alternately.

We now consider a magnon crystal state. The maximal density of independent localized magnons on a kagome lattice is $N_{\text{max}} = \frac{1}{9}N_{\text{sites}}$.²⁹ The magnetization of a plateau is

$$M_{\text{plateau}} = SN_{\text{sites}} + \left(\frac{1}{9}N_{\text{sites}}\right)(-1) = N_{\text{sites}}\left(S - \frac{1}{9}\right). \quad (1)$$

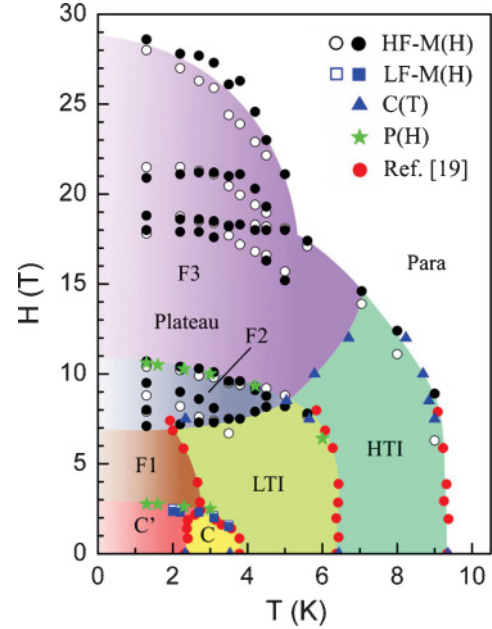


FIG. 3. (Color online) H - T phase diagram for $H \parallel a$ determined from the high-field magnetization (HF-M), electrical polarization (P), specific heat (C), and low-field magnetization (LF-M) measurements. Open (solid) symbols are for increasing (decreasing) field. The red (dark gray) circles are reproduced from Ref. 19 for comparison. Several unique magnetic phases are explored in high magnetic fields and are indicated here as F1–F3. For a better view, the C’-F1 transitions are shown by the LF-M data instead of the HF-M results.

We then have

$$\frac{M_{\text{plateau}}}{M_S} = \frac{N_{\text{sites}}\left(S - \frac{1}{9}\right)}{N_{\text{sites}}S} = 1 - \frac{1}{9S}. \quad (2)$$

In the case of $S = \frac{1}{2}$, the magnon crystal yields a 7/9-magnetization plateau.²⁹ For $S = 1$, this will give a plateau of 8/9, which is in good agreement with our highest magnetization transition. However, from this theory we could not expect magnetization plateaus at $m = 2/3$ and $3/4$. If the spins at $m = 2/3$ have collinear arrangements with fixed length, then an ‘‘up-up-up-up-down’’ spin configuration will be expected to yield $2/3M_S$, which means the magnetic periodicity n should be at least 6. Similarly, n should be 24 for $m = 3/4$ and 18 for $m = 8/9$ in this case. This indicates that long-range interactions beyond the next-nearest-neighbor interaction should also be considered in this system.

Figure 2 shows the temperature dependence of the derivative of magnetization dM/dH [Fig. 2(a)] and the field dependence of the specific heat C/T [Fig. 2(b)] for $H \parallel a$. It is evident that the first transition H_{c1} is of first order. It vanishes at 3.5 K as T increases. H_{c2} and H_{c3} develop well with T and converge at 5 K. H_{c4} and H_{c5} are almost T independent, while H_{c6} is T dependent. The $H = 0$ specific-heat data exhibit the four phase (HTI, LTI, C, and C’) transitions at 9.3, 6.4, 3.6, and 2.3 K, which are in agreement with those in the literature.¹⁹ Magnetic-field-dependent anomalies are observed up to 12 T. The resulting H - T phase diagram is summarized in Fig. 3. It is found that our high-field phase diagram combines very

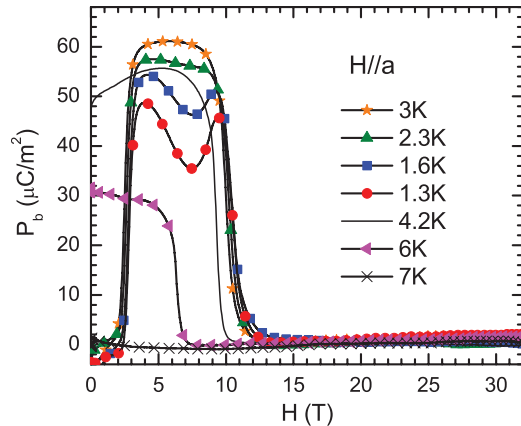


FIG. 4. (Color online) Electrical polarization along the b axis (P_b) at various temperatures measured with increasing H field. During the experiments, an electric field (E) of 10 kV/cm was applied to align the ferroelectric domains as follows: In the ferroelectric LTI phase, E was applied as the sample was cooled down through the transition temperature and removed before the measurement. In the paraelectric phases, E was applied before and persisted during the pulse. The small initial nonzero component and upward trend at high fields are caused by insufficient compensation of background in pulsed fields.

well with previous low-field results. In particular, five unique magnetic phase regions have been explored, including the 1/2-plateau phase. Since the three high-field phases have not been clearly understood, we assign them as a single unknown phase of F3 in the present work and label the other two low-field phases as F1 and F2.

The phase diagrams of anisotropic antiferromagnets have a common feature. The high- and low-field phases are usually separated from a disordered phase by two second-order lines which meet at a multicritical point. Below this point, the two phases can meet at a first-order transition or go into an intermediate mixed phase.³⁰ This multicritical phenomenon is clearly seen in Fig. 3, namely, the F2 phase is an intermediate phase. In other words, the appearance of this phase is due to competition involving two magnetic order parameters. The HTI-LTI phase transition has been determined by the early neutron diffraction measurement corresponding to the ordering of cross-tie spins,³ which was later confirmed by a muon-spin relaxation study.³¹ In this respect, we assume that the LTI-F2 or HTI-F3 transitions are due to the field induced magnetic order of the cross-tie spins. This, in turn, confirms that the 1/2-plateau phase has spin correlation with the cross-tie spins. This correlation must be strong enough, otherwise the cross-tie spins would get easily magnetized in a field which leads to a 1/3 plateau, assuming the spine sites are still ordered as a spiral.

It was revealed that magnetic fields along a will improve the spontaneous electric polarization along b (P_b) of the LTI phase.³ To identify the magnetoelectric properties of the high-field states, we measured P_b as a function of magnetic field up to high fields and show the data in Fig. 4. Different behavior is observed at various temperatures. In the HTI phase, no polarization is detected. In the LTI phase, P_b is strongly suppressed at a critical field, and then disappears. In phases C and C', field induced polarizations are detected in a finite

field range. As T varies, the observed polarizations have a maximal value of 60 $\mu\text{C}/\text{m}^2$ at 3 K. The transition fields are found to coincide with the magnetic phase boundaries, as seen by comparison with the phase diagram of Fig. 3, confirming the coupling between magnetic and ferroelectric order. These results demonstrate that the high-field phase of F3 is paraelectric, which is different from the ferroelectric states F1 and F2. An interesting observation in this study is the unbalance of P_b at very low temperature, which is probably due to the magnetoelectric interactions between the nonequivalent spine and cross-tie spins. DM interactions would lead to further to moments along the b or c axes on the spine sites and make the spiral unstable.

The absence of polarization suggests that the 1/2-plateau phase is not a spiral spin structure as in the LTI phase, but a collinear or coplanar spin arrangement, analogous to that of CuFeO_2 .¹⁰ This change in spin structure is accompanied by a lattice distortion that breaks the spatial inversion symmetry, although it could be very small. In the M - H curve, we see a considerable hysteresis at $H_{c2} < H < H_{c4}$, covering the 1/2 plateau. This hysteresis vanishes at 5 K, corresponding to the multicritical point. A similar magnetization hysteresis was observed before the appearance of this plateau in a static field.³² This scenario is reminiscent of the magnetization plateaus induced by spin-lattice coupling in CuFeO_2 ,¹⁰ CdCr_2O_4 ,⁹ and other frustrated magnets. This spin-lattice coupling effect also exists in the C'-F1 transition because this transition vanishes at T_{C-LTI} , where the thermal expansion study showed abrupt changes in three crystallographic axes.³³ These results confirm that the lattice of NVO is very sensitive to the spin structures of these field induced magnetic states. This conclusion is supported by a recent magnetoelastic study on the four magnetic phases in zero field.³⁴

To summarize, we have performed comprehensive high magnetic field studies on NVO single crystals by measurements of magnetization, electric polarization, and specific heat, and obtained an overall H - T phase diagram for the magnetic easy axis. Many different magnetic phases have been explored in the high magnetic fields. We experimentally observe a half-magnetization plateau and fractional magnetization transitions in this distorted kagome-lattice compound, and point out that the effect of spin-lattice coupling plays an essential role in this process. The obtained H - T phase diagram provides clues for understanding the exchange interactions and the magnetoelectric coupling in this complex spin system; this contributes to a better understanding of recent experimental results. This Rapid Communication also brings a challenge for theoreticians and calls for further neutron diffraction experiments under high magnetic fields to clarify the magnetism of the unusual half-magnetization plateau and other high-field states.

We are grateful to N. Kawashima, T. Suzuki, M. Kenzelmann, and H. Tsunetsugu for useful discussions, and thank F. Herlach for help with the manuscript. This work was supported by a Grant-in-Aid for Scientific Research on priority Areas "High Field Spin Science in 100T" (No. 451) from the Ministry of Education, Culture, Sports, Science and Technology (MEXT). J.W. also acknowledges support from NSFC (Grant No. 10904044).

- ¹C. Broholm, G. Aeppli, G. P. Espinosa, and A. S. Cooper, *Phys. Rev. Lett.* **65**, 3173 (1990).
- ²H. D. Zhou, B. W. Vogt, J. A. Janik, Y.-J. Jo, L. Balicas, Y. Qiu, J. R. D. Copley, J. S. Gardner, and C. R. Wiebe, *Phys. Rev. Lett.* **99**, 236401 (2007).
- ³G. Lawes, A. B. Harris, T. Kimura, N. Rogado, R. J. Cava, A. Aharony, O. Entin-Wohlman, T. Yildirim, M. Kenzelmann, C. Broholm, and A. P. Ramirez, *Phys. Rev. Lett.* **95**, 087205 (2005).
- ⁴L. Seabra and N. Shannon, *Phys. Rev. Lett.* **104**, 237205 (2010).
- ⁵M. Oshikawa, M. Yamanaka, and I. Affleck, *Phys. Rev. Lett.* **78**, 1984 (1997).
- ⁶Y. Narumi, M. Hagiwara, R. Sato, K. Kindo, H. Nakano, M. Takahashi, *Physica B* **246-247**, 509 (1998).
- ⁷N. Okazaki, J. Miyoshi, and T. Sakai, *Physica B* **281-282**, 659 (2000).
- ⁸H. Nakano and M. Takahashi, *J. Phys. Soc. Jpn.* **67**, 1126 (1998).
- ⁹H. Ueda, H. A. Katori, H. Mitamura, T. Goto, and H. Takagi, *Phys. Rev. Lett.* **94**, 047202 (2005).
- ¹⁰N. Terada, Y. Narumi, K. Katsumata, T. Yamamoto, U. Staub, K. Kindo, M. Hagiwara, Y. Tanaka, A. Kikkawa, H. Toyokawa, T. Fukui, R. Kanmuri, T. Ishikawa, and H. Kitamura, *Phys. Rev. B* **74**, 180404 (2006).
- ¹¹T. Inami, Y. Ajiro, and T. Goto, *J. Phys. Soc. Jpn.* **65**, 2374 (1996).
- ¹²T. Ono, H. Tanaka, H. A. Katori, F. Ishikawa, H. Mitamura, and T. Goto, *Phys. Rev. B* **67**, 104431 (2003).
- ¹³K. Hida, *J. Phys. Soc. Jpn.* **70**, 3673 (2001).
- ¹⁴K. Damle and T. Senthil, *Phys. Rev. Lett.* **97**, 067202 (2006).
- ¹⁵A. Sen, K. Damle, and A. Vishwanath, *Phys. Rev. Lett.* **100**, 097202 (2008).
- ¹⁶K. Okuta, S. Hara, H. Sato, Y. Narumi, and K. Kindo, *J. Phys. Soc. Jpn.* **80**, 063703 (2011).
- ¹⁷Y. Okamoto, M. Tokunaga, H. Yoshida, A. Matsuo, K. Kindo, and Z. Hiroi, *Phys. Rev. B* **83**, 180407(R) (2011).
- ¹⁸T. Matsushita, N. Hamaguchi, K. Shimizu, N. Wada, W. Fujita, K. Awaga, A. Yamaguchi, and H. Ishimoto, *J. Phys. Soc. Jpn.* **79**, 093701 (2010).
- ¹⁹M. Kenzelmann, A. B. Harris, A. Aharony, O. Entin-Wohlman, T. Yildirim, Q. Huang, S. Park, G. Lawes, C. Broholm, N. Rogado, R. J. Cava, K. H. Kim, G. Jorge, and A. P. Ramirez, *Phys. Rev. B* **74**, 014429 (2006).
- ²⁰I. Cabrera, M. Kenzelmann, G. Lawes, Y. Chen, W. C. Chen, R. Erwin, T. R. Gentile, J. B. Leao, J. W. Lynn, N. Rogado, R. J. Cava, and C. Broholm, *Phys. Rev. Lett.* **103**, 087201 (2009).
- ²¹V. Ogloblichev, K. Kumagai, S. Verkhovskii, A. Yakubovskiy, K. Mikhalev, Yu. Furukawa, A. Gerashenko, A. Smolnikov, S. Barilo, G. Bychkov, and S. Shiryayev, *Phys. Rev. B* **81**, 144404 (2010).
- ²²F. Fabrizi, H. C. Walker, L. Paolasini, F. De Bergevin, T. Fennell, N. Rogado, R. J. Cava, Th. Wolf, M. Kenzelmann, and D. F. McMorrow, *Phys. Rev. B* **82**, 024434 (2010).
- ²³R. C. Rai, J. Cao, S. Brown, J. L. Musfeldt, D. Kasinathan, D. J. Singh, G. Lawes, N. Rogado, R. J. Cava, and X. Wei, *Phys. Rev. B* **74**, 235101 (2006).
- ²⁴Z. Z. He, Y. Ueda, and M. Itoh, *J. Cryst. Growth* **297**, 1 (2006).
- ²⁵Note that the dM/dH curves were derived directly from the dM/dt data by our induction method, which means these anomalies in dM/dH curves are intrinsic. Magnetic studies indicated that the para-HTI and HTI-LTI transitions produced almost invisible anomalies in susceptibility. Hence, we believe these anomalies are due to the magnetic transitions.
- ²⁶T. Yildirim, L. I. Vergara, J. Iniguez, J. L. Musfeldt, A. B. Harris, N. Rogado, R. J. Cava, F. Yen, R. P. Chaudhury, and B. Lorenz, *J. Phys. Condens. Matter* **20**, 434214 (2008).
- ²⁷H. Nakano and T. Sakai, *J. Phys. Soc. Jpn.* **79**, 053707 (2010).
- ²⁸K. Hida, *J. Phys. Soc. Jpn.* **69**, 4003 (2000).
- ²⁹M. E. Zhitomirsky and H. Tsunetsugu, *Prog. Theor. Phys. Suppl.* **160**, 361 (2005); *Phys. Rev. B* **70**, 100403(R) (2004).
- ³⁰A. D. Bruce and A. Aharony, *Phys. Rev. B* **11**, 478 (1975).
- ³¹T. Lancaster, S. J. Blundell, P. J. Baker, D. Prabhakaran, W. Hayes, and F. L. Pratt, *Phys. Rev. B* **75**, 064427 (2007).
- ³²N. R. Wilson, O. A. Petrenko, and G. Balakrishnan, *J. Phys. Condens. Matter* **19**, 145257 (2007).
- ³³R. P. Chaudhury, F. Yen, C. R. dela Cruz, B. Lorenz, Y. Q. Wang, Y. Y. Sun, and C. W. Chu, *Phys. Rev. B* **75**, 012407 (2007).
- ³⁴L. I. Vergara, J. Cao, N. Rogado, Y. Q. Wang, R. P. Chaudhury, R. J. Cava, B. Lorenz, and J. L. Musfeldt, *Phys. Rev. B* **80**, 052303 (2009).